Experimental studies on the motion of a flexible hydrofoil

By H. R. KELLY, A. W. RENTZ
U.S. Naval Ordnance Test Station, China Lake, California
AND J. SIEKMANN
University of Florida, Gainesville, Florida

(Received 4 October 1963)

A thin, flexible hydrofoil has been used as a model to simulate the swimming of a two-dimensional fish in an ideal, incompressible fluid, as treated in recent theoretical papers. The apparatus is described in some detail and typical data are compared with the predictions of theory. An error analysis is given, showing that, within the expected errors and limits of validity of theory, experimental verification of theory is very good.

1. Introduction

A few years ago investigations regarding the locomotion of aquatic animals were initiated at the U.S. Naval Ordnance Test Station (NOTS), China Lake, California. Although the Navy-sponsored research comprises many fields, the present paper is chiefly concerned with a series of experiments that were conducted by NOTS at the California Institute of Technology Hydrodynamics Laboratory in order to check the validity of recent theoretical studies on fish propulsion. Some results of this paper have been briefly reported previously by one of the authors (Kelly 1961) without, however, a detailed discussion of the experimental work, which represents a substantial part of the NOTS sea animal locomotion program.

It is not expected that the results reported here will apply to a living fish in three-dimensional flow, but will merely confirm the validity of the two-dimensional theory that has been compiled so far.

2. Theoretical results

During recent years several theoretical contributions dealing with the hydrodynamics of fish propulsion have appeared in the literature (Smith & Stone 1961; Wu 1961; Siekmann 1962*a*, *b*, 1963). Although the methods used are different, it can be shown that the results are almost identical. This is not surprising, since all these investigations are based on linearized theory, using as a model for the simulation of the locomotion of sea animals essentially a thin, undulating, flexible hydrofoil in two-dimensional, inviscid and incompressible flow. The assumptions underlying the theoretical developments can be formulated as follows.

(i) The waving plate is two-dimensional, extending along the x-axis of a right-hand Cartesian co-ordinate system from $x = -1$ to $x = +1$, and immersed in an otherwise uniform stream of constant velocity U in the positive x-direction;

(ii) the thickness of the plate is zero;

(iii) the displacement of the plate in the y-direction is small compared to the length; therefore the maximum amplitude and slope of the transverse motion are small compared to unity;

(iv) the perturbation velocities due to the motion of the plate are small compared to the free-stream velocity.

It has been pointed out that this last assumption is not really an essential one, since the linearized equations may be valid in cases where the perturbations become larger than the free-stream speed. Actually, the assumption that the

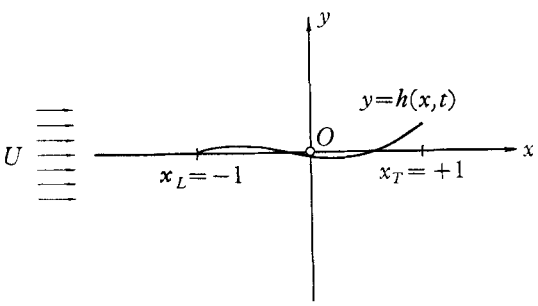

FIGURE 1. Sketch of flexible solid plate in a uniform parallel flow.

wake vorticity remains on axis and that the Kutta condition be valid at the trailing edge will become invalid in almost the same reduced-frequency régimes as the assumptions of small perturbation velocities.

Now we prescribe the motion of the flexible hydrofoil at any time t by

$$y = h(x,t) = f(x)\cos(\alpha x - \beta t + \delta) \quad (-1 \leqslant x \leqslant +1) \tag{1}$$

with the amplitude function $f(x)$, the wave-number α, the circular frequency β, and a phase angle δ (figure 1). It is advantageous to use complex notation and to include equation (1) into the most general form of simple harmonic motion

$$y = g(x,t) = F(x)\,e^{i\beta t} \quad (-1 \leqslant x \leqslant +1), \tag{2}$$

where $F(x)$ may be complex. For a physical interpretation the real part of $g(x,t)$ is to be used. Since the plate is infinitesimally thin, the functions $g(x,t)$ and $\partial g(x,t)/\partial x$ must be even functions of a variable ϑ, which is defined by

$$x = -\cos\vartheta \quad (0 \leqslant \vartheta \leqslant \pi). \tag{3}$$

Then we can express $F(x)$ and its derivative dF/dx as Fourier cosine series in ϑ. Their Fourier coefficients are B_n and C_n, respectively.

The boundary condition of the problem results from the fact that the 'fish' is assumed to be a material, impenetrable body, so that the component of the flow velocity normal to the moving solid boundary must be equal to the velocity of this boundary. Hence, denoting the x and y components of the perturbation

velocities due to the deformation of the plate by $u(x, y, t)$ and $v(x, y, t)$ we arrive, after linearization, at

$$v = U\left[\frac{dF}{dx} + i\omega F\right] e^{i\beta t} \quad \text{on} \quad y = \pm 0 \quad (-1 \leqslant x \leqslant 1), \tag{4}$$

where

$$\omega = \beta/U \tag{5}$$

is the reduced frequency.

Denoting the Fourier coefficients of the 'downwash' $v(x, \pm 0, t) = w(\vartheta, t)$ by A_n, the boundary condition (4) implies the following relation between the coefficients A, B and C,

$$A_n = C_n + i\omega B_n. \tag{6}$$

In order to determine the thrust T acting on the undulating hydrofoil, we have to integrate the product of the pressure difference between the top and bottom sides of the waving plate and the local slope of the plate along the chord line. We further have to add the so-called leading-edge suction force. Taking the time average value of the thrust over a single period $\tau = 2\pi/\beta$, we obtain finally

$$\overset{*}{T} = \frac{1}{\tau}\int_0^\tau T\,dt = \pi\rho U^2\{(a_0' - C_0')(a_0' - C_1') + (a_0'' - C_0'')(a_0'' - C_1'') - \omega^2(B_0' B_1' + B_0'' B_1'')\}, \tag{7}$$

with ρ as the density of the liquid

$$a_0' = \mathfrak{F}(\omega)(A_0' - A_1') - \mathfrak{G}(\omega)(A_0'' - A_1'') + A_1', \tag{8a}$$

$$a_0'' = \mathfrak{F}(\omega)(A_0'' - A_1'') + \mathfrak{G}(\omega)(A_0' - A_1') + A_1'', \tag{8b}$$

and

$$A_0' = \operatorname{Re} A_0, \quad A_0'' = \operatorname{Im} A_0, \text{ etc.} \tag{9}$$

The functions $\mathfrak{F}(\omega)$ and $\mathfrak{G}(\omega)$ in equations (8*a*, *b*) indicate the real and imaginary part of the Theodorsen function

$$\mathfrak{C}(\omega) = \mathfrak{F}(\omega) + i\mathfrak{G}(\omega) = \frac{H_1^{(2)}(\omega)}{H_1^{(2)}(\omega) + iH_0^{(2)}(\omega)}, \tag{10}$$

where $H_0^{(2)}$ and $H_1^{(2)}$ denote the Hankel functions of second kind and zeroth and first order. The thrust coefficient c_T is defined by

$$c_T = \overset{*}{T}/\pi\rho U^2. \tag{11}$$

The above theoretical result has been obtained by two different methods. These are (*a*) that of Wu (1961) using an acceleration-potential technique, and (*b*) that of Siekmann (1962*a*, *b*) postulating a vorticity distribution over the hydrofoil and in the wake and solving the resultant integral equation for the downwash.

To maintain the prescribed motion, an external force equal in magnitude and opposite in sign to the pressure force across the hydrofoil must be applied. The power P required to sustain the motion is equal to the time rate of work done by this external force. Taking again the time average value over a period τ, calculation yields

$$\overset{*}{P} = -\pi\rho U^3\omega\{a_0'(B_0'' + B_1'') - a_0''(B_0' + B_1') + 2\omega(B_0' B_1' + B_0'' B_1'') - (B_0'' C_1' - B_0' C_1'') - (B_1'' C_0' - B_1' C_0'')\}. \tag{12}$$

Again we can define a coefficient, namely the power coefficient,

$$c_P = \overset{*}{P}/\pi\rho U^3. \tag{13}$$

The theory of Smith & Stone is distinct from those of Wu and Siekmann, in that the wake vorticity was neglected. It will be shown by comparison with experiment that this often makes a considerable difference.

3. Experimental results

In order to compare theoretical results with available experimental data, the motion of the hydrofoil was assumed to be of the form

$$y = h(x,t) = \mathrm{Re}\, g(x,t) = \mathrm{Re}\,[(c_0 + c_1 x + c_2 x^2)\, e^{-i\alpha x} e^{i\beta t}]. \tag{14}$$

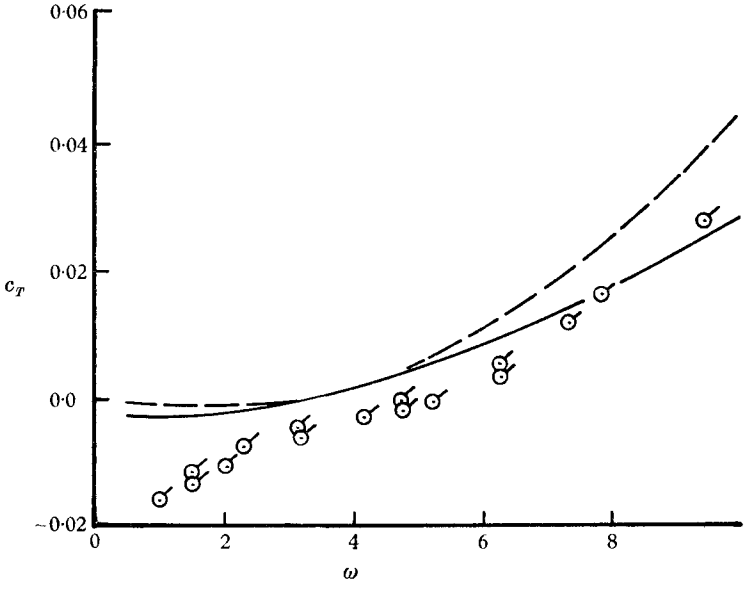

FIGURE 2. Thrust coefficient versus reduced frequency for constant amplitude. $c_0 = \frac{1}{12}$, $c_1 = 0$, $c_2 = 0$, $\alpha = \pi$. Theory: Wu (1961) and Siekmann (1962*a*), ———; Smith & Stone (1961), – – – –. Experiment: metal hydrofoil, ⊙.

The displacement of the plate was made dimensionless by reference to the half-chord L. Therefore, denoting the chord by $2L$ and the finite width of the plate by W, the reduced frequency is†

$$\omega = \beta L/U, \tag{15}$$

while the thrust coefficient is given by†

$$c_T = \overset{*}{T}/\pi\rho U^2 LW. \tag{16}$$

(*a*) *Reduced frequency finite* ($1 < \omega < 10$)

Agreement between experiment and theory was excellent for several cases. As an example, the case of constant amplitude with wavelength equal to plate length ($c_0 = \frac{1}{12}$, $\alpha = \pi$) shows good agreement in the range $3 < \omega < 7$ (figure 2). For this particular case it was observed by means of dye flow patterns that, for

† Cf. Kelly (1961).

$\omega < 3$, flow separation occurred in the lee of the peaks of waves of the plate and that this became progressively worse as ω approached zero. Since the free-stream speed is greater than the wave speed for $\omega < \pi$, the separation is not surprising, and will tend to make the theory less valid, the greater the region of separation. Poor pressure recovery in these stalled areas of the plate gives a rapid increase in drag and thus accounts for the sharp decrease in the thrust coefficient for small ω.

An approximately constant difference

$$c_T^{\text{theory}} - c_T^{\text{experiment}} \sim 0{\cdot}004 \ldots 0{\cdot}006$$

between theory and experiment may be seen in figure 2 for the range $3 < \omega < 7$, which is assumed to be due to viscous drag.

As ω exceeds the value 7, it may be seen from figure 2 that experimental thrust coefficients become larger than the predicted theoretical values. However, in this range of high ω the assumption that the perturbation velocities are small compared with the free-stream velocity is violated to a serious degree, and a noticeable divergence between theory and experiment is not surprising. On the other hand, flow pictures show a rapid sideways diffusion of vorticity in the wake at high frequency. It is not yet known how much this may effect the results.

The experimental thrust coefficients (figures 3*a*, *b*) with quadratic amplitude ($c_0 = 0{\cdot}023$, $c_1 = 0{\cdot}042$, $c_2 = 0{\cdot}034$, $\alpha = \pi$) agree well with Siekmann's theory if corrections are made for a turbulent skin friction drag over the reduced frequency range $1 \leqslant \omega \leqslant 6$ for the metal hydrofoil and $1 \leqslant \omega \leqslant 5$ for the rubber hydrofoil. For $\omega > 6$ the experimental thrust coefficients are larger for the metal hydrofoil and smaller for the rubber hydrofoil than the theoretical value. As pointed out previously, these values of ω are larger than those for which the linearized theory applies and as a consequence theory should not be accepted as completely correct. For the experiments a metal hydrofoil and a rubber hydrofoil were employed where the trailing edge of the first one was $\frac{1}{4}$ in. longer than that of the rubber foil. But the $\frac{1}{4}$ in. extension of the trailing edge of the metal plate only partially explains the difference in thrust between the metal and rubber foil at high reduced frequencies. This leaves the fact that the trailing edge of the metal foil is sharp while the trailing edge of the rubber foil is rounded ($\frac{1}{16}$ in. radius) to explain the remaining thrust advantage of the metal foil at high reduced frequencies. Almost all fish have a sharp trailing edge. As noted from the data in figure 2, drag-producing flow separation occurred for $\omega < 3$ as ω tended to zero. This does not happen for the quadratic amplitude, at least not down to $\omega > 1$. This particular quadratic wave-form was derived from movies of a salmon swimming in a flume. The possibility exists that proper amplitude variation with length lessens the chances for flow separation on a fish body as he coasts along in the non-propulsive condition ($\omega < \pi$). This is only a suggestion, since it is realized that three-dimensional flow is essentially different from that in two dimensions.

The case of a flat plate ($c_0 = \frac{1}{24}$, $\alpha = 0$) undergoing an oscillation normal to the flow with no rotation is presented in figure 4. It shows excellent agreement between experiment and theory over the entire range of reduced frequency.

One of the reasons for this good agreement may be the small amplitude used here, which permitted the machine to fulfil more nearly the requirements of two-dimensional flow.

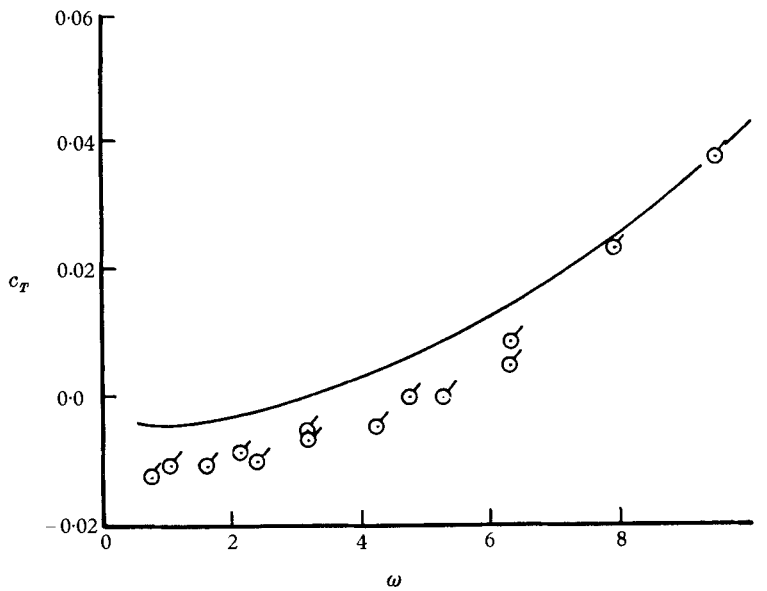

FIGURE 3*a*. Thrust coefficient versus reduced frequency for quadratic amplitude. $c_0 = 0{\cdot}023$, $c_1 = 0{\cdot}042$, $c_2 = 0{\cdot}034$, $\alpha = \pi$. Theory: Siekmann (1962*a*), ———. Experiment: metal hydrofoil, ⊙.

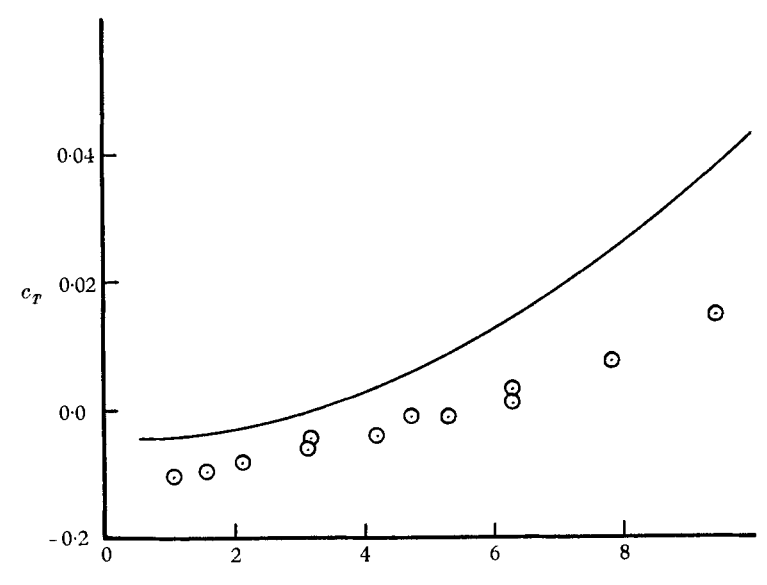

FIGURE 3*b*. Thrust coefficient versus reduced frequency for quadratic amplitude. $c_0 = 0{\cdot}023$, $c_1 = 0{\cdot}042$, $c_2 = 0{\cdot}034$, $\alpha = \pi$. Theory: Siekmann (1962*a*), ———. Experiment: rubber hydrofoil, ⊙.

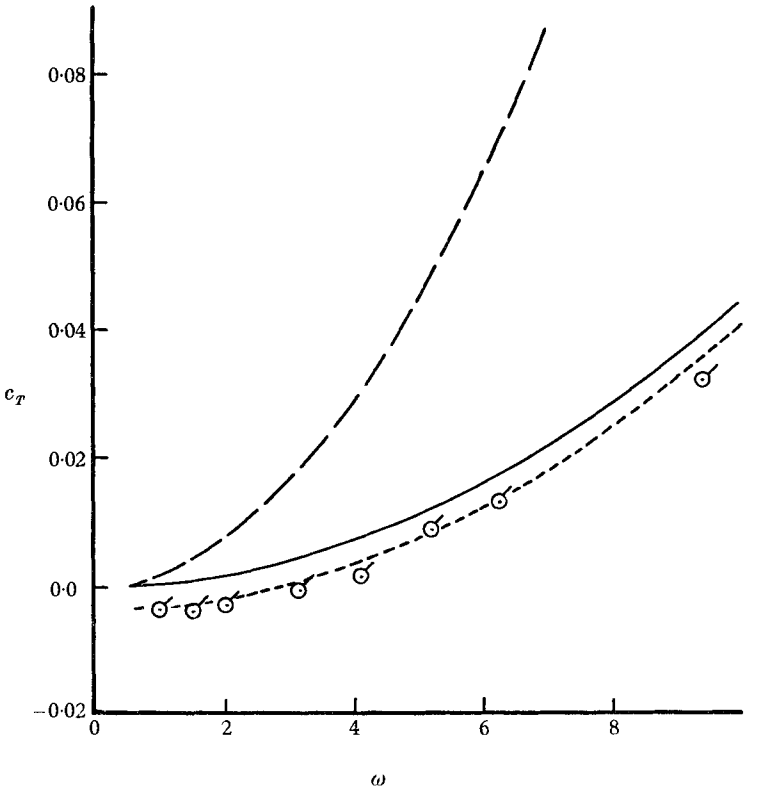

FIGURE 4. Thrust coefficient versus reduced frequency for a rigid flat plate. $c_0 = \frac{1}{24}$, $c_1 = 0$, $c_2 = 0$, $\alpha = 0$. Theory: Siekmann (1963), ———; Smith & Stone (1961), — — —: turbulent boundary-layer drag added to Siekmann's (1963) result, – – – –. Experiment: metal hydrofoil, ⊙.

(*b*) *Reduced frequency infinite* ($\omega \to \infty$ as $U \to 0$)

For this case good agreement between theory and experiment should not be expected. Wu and Siekmann arrived at a theoretical prediction of thrust coefficients for $U = 0$ by taking the limiting value of c_T with $\beta = \omega U$ held constant as U tends to zero, i.e.

$$\bar{c}_T = \lim_{\substack{U \to 0 \\ \beta = \text{const.}}} (\mathring{T}/\pi\rho\beta^2). \tag{17}$$

Of course, the linearizing assumption that the perturbation velocities are small in comparison to the free-stream velocity does not hold if U approaches zero.

For the constant amplitude case ($c_0 = \frac{1}{24}$, $\alpha = \pi$) experimental values were several times as large as theory (figure 5). The spread in experimental thrust coefficients at low frequencies β is caused by a small constant-magnitude error in the measurement of thrust during the two different runs. As β increases and thrust increases the size of this error becomes small in comparison to the gross thrust output and the thrust coefficients computed from the two runs approach the same value.

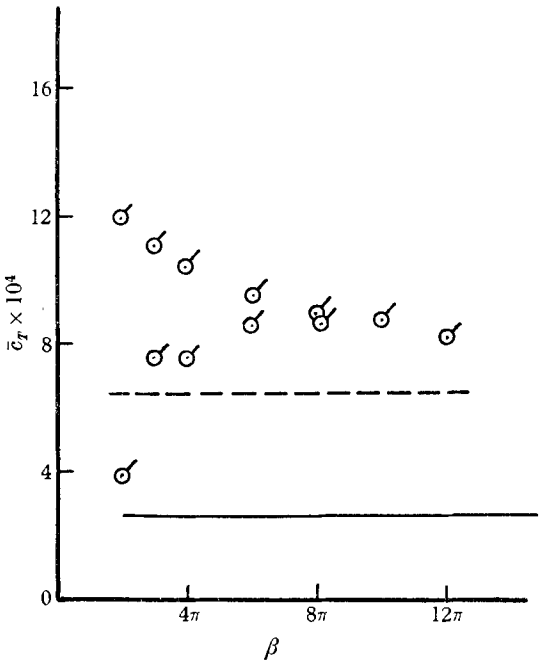

FIGURE 5. Thrust coefficient versus circular frequency for constant amplitude and $U = 0$. $c_0 = \frac{1}{24}$, $c_1 = 0$, $c_2 = 0$, $\alpha = \pi$. Theory: Siekmann (1963), ———; Smith & Stone (1961), – – – –. Experiment: metal hydrofoil, ⊙.

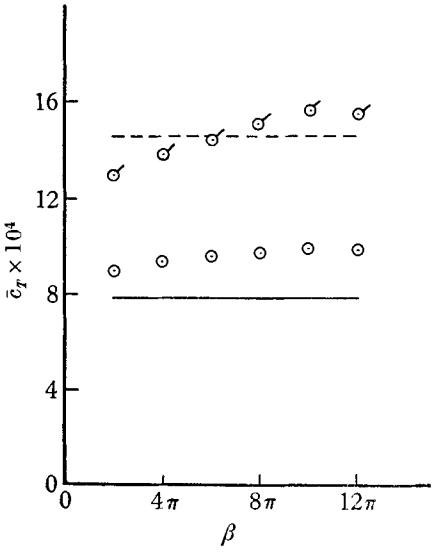

FIGURE 6(*a*)

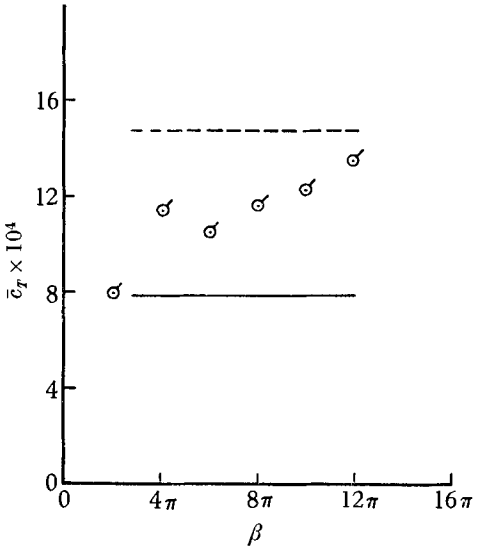

FIGURE 6(*b*)

FIGURE 6*a* Thrust coefficient versus circular frequency for linear amplitude and $U = 0$. $c_0 = \frac{1}{16}$, $c_1 = \frac{1}{16}$, $c_2 = 0$, $\alpha = \pi$. Theory: Siekmann (1963), ———; Smith & Stone (1961), – – – –. Experiment: rubber hydrofoil, ⊙; metal hydrofoil, ⊙.

FIGURE 6*b*. Thrust coefficient versus circular frequency for linear amplitude and $U = 0$. $c_0 = \frac{1}{16}$, $c_1 = \frac{1}{16}$, $c_2 = 0$, $\alpha = \pi$. Theory: Siekmann (1963), ———; Smith & Stone (1961), – – – –. Experiment: metal hydrofoil, ⊙; $\frac{1}{4}$ in. trimmed from trailing edge.

For the linear amplitude case ($c_0 = \frac{1}{16}$, $c_1 = \frac{1}{16}$, $\alpha = \pi$) agreement is best when using a rubber hydrofoil (figure 6*a*). All experimental data calculations were made for a plate 12 in. long. The metal plate was actually $12\frac{1}{4}$ in. long. Trimming $\frac{1}{4}$ in. from the trailing edge of the plate produced the reduction in the thrust coefficient (figure 6*b*). The remaining difference between the thrust coefficients of the metal

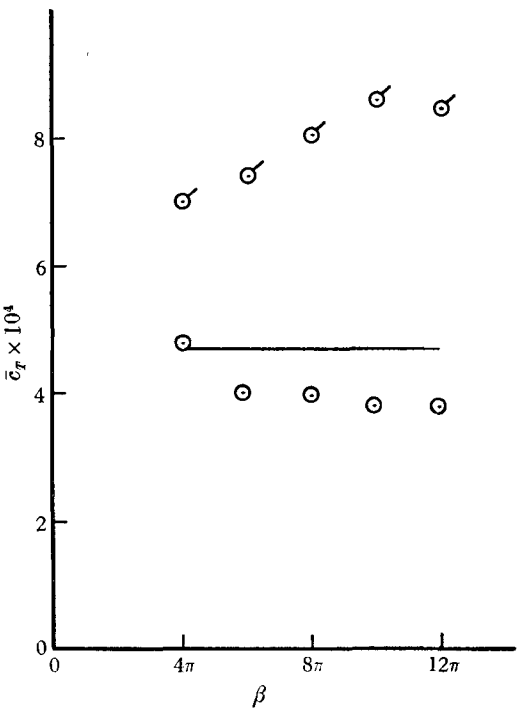

FIGURE 7. Thrust coefficient versus circular frequency for quadratic amplitude and $U = 0$. $c_0 = 0{\cdot}023$, $c_1 = 0{\cdot}042$, $c_2 = 0{\cdot}034$, $\alpha = \pi$. Theory: Siekmann (1963). Experiment: metal hydrofoil, ⊙; rubber hydrofoil, ⊙.

and rubber hydrofoils should probably be attributed to the sharp trailing edge of the metal foil as against the rounded edge of the rubber hydrofoil.

For the quadratic amplitude ($c_0 = 0{\cdot}023$, $c_1 = 0{\cdot}042$, $c_2 = 0{\cdot}034$, $\alpha = \pi$) shown in figure 7 agreement is good for the rubber hydrofoil but not for the metal hydrofoil.

4. Experimental apparatus

The test machine was designed and built by G. Bowlus of NOTS, Pasadena. It consisted of a flexible flat hydrofoil 12 in. long by 4 in. wide mounted horizontally between two vertical walls in an 'H' configuration. The most suitable models tried were made of $\frac{1}{8}$ in. thick moulded rubber. Transverse stiffening was provided by rods imbedded in the rubber. It should will be noted that the rod imbedded in the leading edge was longer. It also was hollow to allow the introduction of dye. The walls were hollow and contained seven pairs of driver arms that gripped the rods projecting from the edge of the plate through slots in the wall, and the arms were also attached to a reciprocating mechanism above. The amplitude and phasing of the reciprocating arms could be adjusted, making

it possible to generate a wide variety of travelling waves. The thrust of the hydrofoil was absorbed by the forward pair of drivers, which were held yoke-fashion by a pair of arms attached to a rigid rectangle above. This was suspended from the main frame by means of flexural pivots, permitting it, along with the plate, to swing freely in the fore- and aft-direction. A 3 ft. long rod connected this system to a three-component balance located downstream from the test apparatus in the California Institute of Technology free surface water tunnel. The balance had a sensitivity of $\pm 0{\cdot}001$ lb. Because of friction in the test apparatus under optimal operating conditions, the over-all sensitivity was never better than $\pm 0{\cdot}003$ lb.; on some tests it was $\pm 0{\cdot}010$ lb., and on a few poor tests $\pm 0{\cdot}030$ lb. During the first two series of tests the mechanical balance was used exclusively for measuring the thrust output. During the third test period a Statham strain gauge was hooked in series with the mechanical balance. The output was fed into a CEC type 351 galvanometer mounted in a CEC type 119 recording oscillograph. The shunt circuit was adjusted to give a flat response from 0 to 12 c/s. The mechanical balance was used to calibrate the strain gauge. Another galvanometer was hooked up to a contact switch which was closed once per cycle and recorded on the oscillograph record. This permitted correlation between thrust output and wave phase in the plate.

Since power-absorbed data were desired for the plate also, the torque output of the motor was measured. The motor was mounted on ball bearings and the torque restraint supplied by a single-leaf flex spring. Over the range of interest the angular deflexion of the motor was directly proportional to its torque output. A light beam reflected from a prism mounted on the motor axis to a scale mounted about 6 ft. away provided a readout for the torque.

On the last series of tests the motor mount was the same; however, the torque restraint was supplied by a rigid arm that hooked to a strain gauge whose output was recorded on the CEC 119 oscillograph. A small weight suspended from known points on the arms supplied the calibration for the strain gauge. The output of a tachometer generator driven by the machine was hooked to a Berkeley counter to provide accurate determination of the period of oscillation of the hydrofoil. Water tunnel flow velocity was measured by a 1 in. diameter, five-bladed plastic propeller mounted in jewelled bearing and having a specific gravity of one. The rotational rate of this propeller was measured by electronic circuitry which sensed the change in resistivity as each blade passed a copper electrode. This apparatus was constructed for the sea animal locomotion programme by M. Slater of the water tunnel staff of the California Institute of Technology. Two small dye-ejection holes were located on the top and bottom of the plate at the leading edge. Potassium perchlorate dissolved in water was fed into the hollow leading edge by an external pressure system.

For one series of tests a 13-prong Pitot rake was set up downstream of the plate and a survey of total pressure versus vertical displacement from the plate centreline conducted. In figure 8, plate 1, one may see the Pitot rake in place in the tunnel, along with the experimental apparatus, including the mechanical balance (upper left). Photographic coverage was supplied by 35 mm Mitchell movie cameras with 1000 cycle binary coded time recorded on the film edge. A number

of shots of flow patterns were taken using black and white film in a 4×5 press camera. Resolution of this camera film combination was much better than that of the 35 mm movie camera.

5. Test procedure

The hydrofoil was set to the desired wavelength and wave amplitude in the machine prior to being placed in the tunnel. It was then placed in the water tunnel and hooked up to the mechanical balance, recording oscillograph, dye-injection mechanism, and driving motor, which was bolted to the tunnel.

The tunnel test section was next flooded with water to insure that all sliding parts which operated under water would be lubricated with water. The tunnel was then drained and the zero thrust and torque calibration runs commenced. Normally the model would be operated at about 3 c/s and the machine then operated at 1, 2, 3, 4, 5, and 6 c/s, and the torque required to drive the machine recorded by the prism-deflected light beam. When strain gauges were being used to record thrust, the gauges were loaded by the mechanical balance to 0·0, 0·05, 0·1, 0·2, 0·3, 0·5, and 1·0 lb. and the light beam deflexion of the galvanometer connected to the thrust output strain gauge recorded with the CEC 119 oscillograph. Likewise for the torque arm, torques of 0, 1, 2, 3 and 4 in.-lb. were applied and the resulting light beam deflexion recorded by the oscillograph.

Once the calibration procedure was finished, the tunnel was refilled with water and measurements of thrust and torque made with tunnel flow velocity set successively to 0, 1, 2, and 3 ft./sec and machine frequency to 1, 2, 3, 4, 5, and 6 c/s for each flow velocity. This gave a total of 24 data points per wave-form for thrust and 24 data points per wave-form for torque. After a set of data points were recorded for each flow velocity, a check of zero points for thrust and torque was made to guarantee that no drift had occurred. Care was taken to see that both water velocity and frequency were accurate to within 1 %. Thrust varied rapidly with frequency. A small drift in frequency produced a noticeable error in measured thrust

6. Data reduction

Since theory indicated that the thrust and power coefficients (equations (11) and (13)) were essentially functions of the reduced frequency ω, all experimental data were reduced to coefficient form in order to permit a more concise presentation of the results as functions of ω.

Thrust data from the mechanical balance were corrected for zero error and reduced directly to coefficient form.

Thrust data from strain gauges recorded by the oscillograph in the form of force versus time were integrated over one cycle to obtain an average curve height. This average height was multiplied by the calibration factor to give the time-averaged thrust. Then the time-averaged thrust was used to compute the thrust coefficient.

A typical thrust versus time curve is shown in figures 9*a*, *b*. The net time-averaged thrust is proportional to the area between the solid curve and the dotted, no-water curve.

The best torque data were taken from the strain-gauge records, two samples of which are shown in figure 10. The area under the curve was integrated over one cycle and then divided by the physical length of one cycle to give the time-averaged height of the curve. This was multiplied by a calibration factor to obtain the time-averaged torque. This procedure was repeated for all the different points to yield curves of torque versus frequency for the velocities of 0, 1, 2,

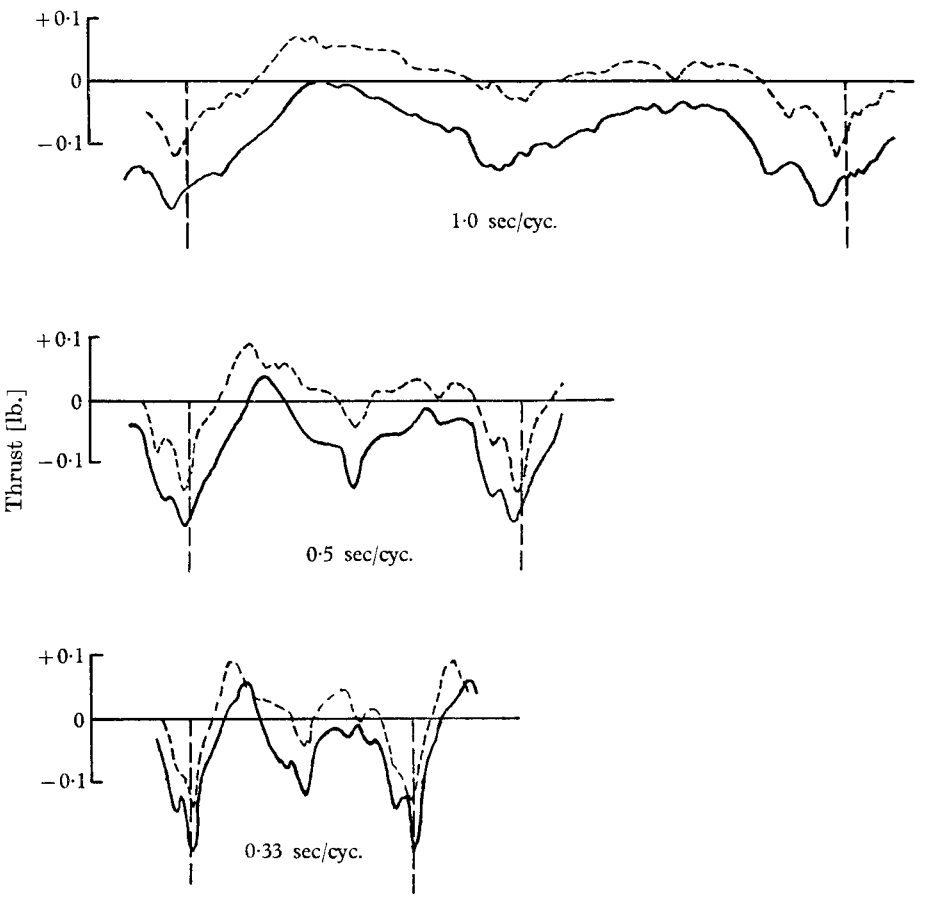

FIGURE 9*a*. Thrust versus time over one cycle (strain gauge) for quadratic amplitude. $c_0 = 0{\cdot}023$, $c_1 = 0{\cdot}042$, $c_2 = 0{\cdot}034$, $\alpha = \pi$. $U = 3$ ft./sec, ———; no water, – – – –.

and 3 ft./sec and for the case of no water around the plate (figure 11). It was assumed that the difference between the 'no water' torque curve and a particular torque-velocity curve at a given frequency represents the torque required to drive the plate in water at that particular flow velocity and wave velocity. This procedure was used to derive the data in figure 12. The torque required to drive the machine ranged from 3 to 100 times that required to operate the plate in water with the range of values being 20 to 100 times in the reduced-frequency range of most interest. To derive the plate torque, the difference between the two large machine torques had to be taken. This, coupled with the fact that the

torque required to operate the machine in air was a slightly variable quantity due to dust particles contaminating bearings, leads to large uncertainties in the derived power curves.

Theory predicted that plate power required went to zero when the plate wave velocity equalled the water flow velocity. A curve was faired through a given torque-velocity set of data and the no-water torque curve moved vertically until

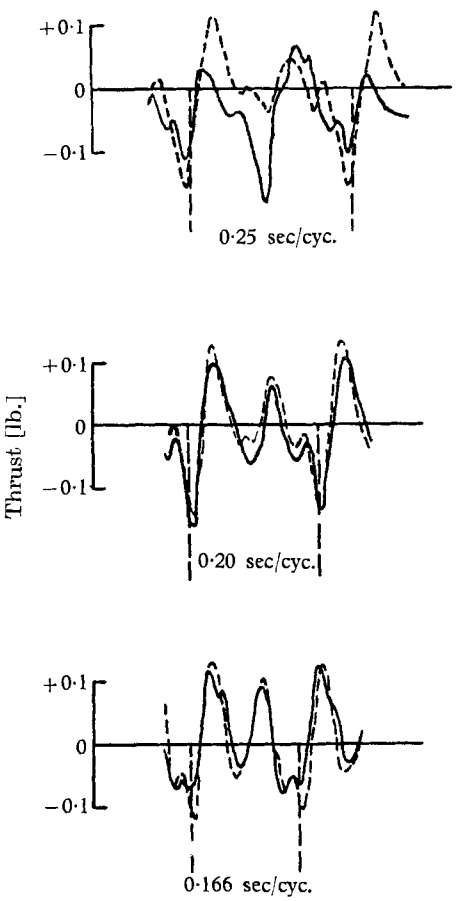

FIGURE 9*b*. Thrust versus time over one cycle (strain gauge) for quadratic amplitude. $c_0 = 0{\cdot}023$, $c_1 = 0{\cdot}042$, $c_2 = 0{\cdot}034$, $\alpha = \pi$. $U = 3$ ft./sec, ———; no water, – – – –.

it intersected the torque-velocity curve at the zero-power-required point predicted by theory. This sort of manipulation resulted in the apparent agreement between experimental and theoretical power coefficients as shown for example in figure 13.

The first and second series of tests used a 0·010 in. beryllium-bronze hydrofoil that was subjected to considerable transverse bending. This pushed the driver arms against the plastic walls and possibly affected the thrust and power readings of the machine to a certain degree. The last series of tests utilized a molded rubber hydrofoil of approximately $\frac{1}{8}$ in. thickness with transverse stiffening

rods. This rubber plate with the rigid rods completely spanning the gap between pairs of driver arms, almost eliminated the aforementioned problem.

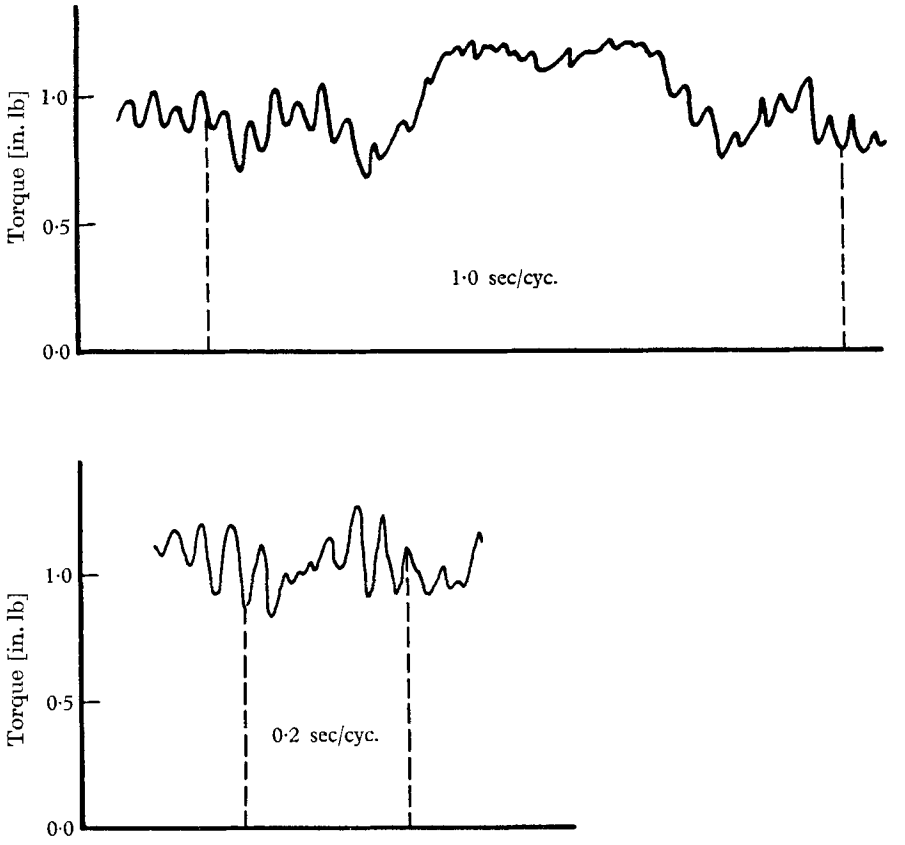

FIGURE 10. Total torque versus time over one cycle (strain gauge) for quadratic amplitude $c_0 = 0{\cdot}023$, $c_1 = 0{\cdot}042$, $c_2 = 0{\cdot}034$, $\alpha = \pi$. $U = 1$ ft./sec.

7. Error analysis

For thrust measurements using the rubber hydrofoil and with wave amplitudes of $\frac{1}{2}$ in. or less, the standard deviation was of the order 0·002 lb. Using a metal hydrofoil, it was found for the linearly varying amplitude that this value was closer to 0·010 lb. Likewise, the zero point was determined to $\pm$ 0·002 lb., which results in additional uncertainties equal in magnitude to those due to thrust measurement errors. With regard to the larger amplitudes, we found that the accuracy of an individual data point ranged from $\pm$ 0·003 to $\pm$ 0·010 with correspondingly larger random errors in the values of c_T. The largest errors, however, are those which either were not or could not be evaluated. They are:

(*a*) *Free-surface effect*

For the case $U = 0$, $c_0 = c_1 = \frac{1}{16}$, and $\beta = 6\pi$, a 15 % increase in thrust was noted when the surface immediately above the plate was restrained by holding a sheet of plastic on the water surface, thus preventing surface deformities. No systematic evaluation of this effect was attempted.

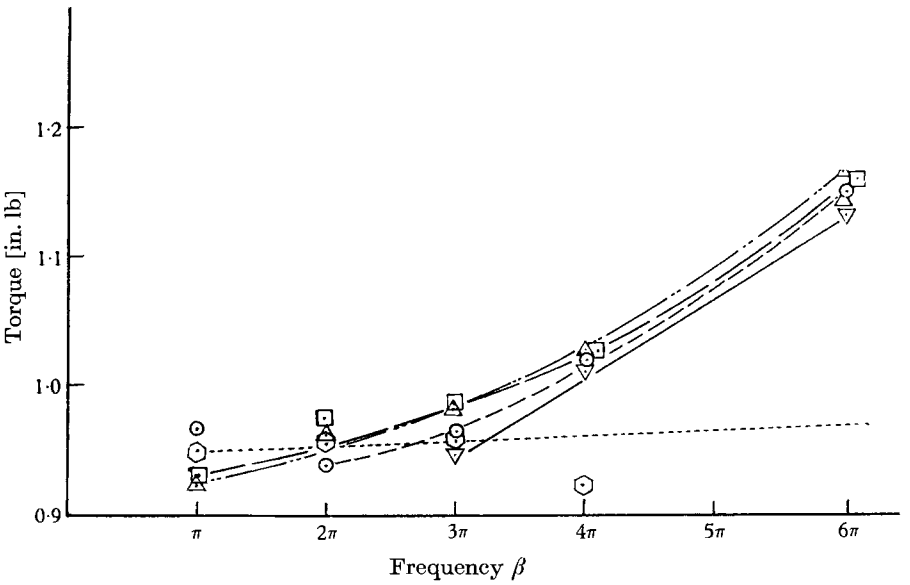

FIGURE 11. Total torque versus frequency for quadratic amplitude. ⊙, – – – –, no water (machine torque); ⊙, – – – –, $U = 0$ ft./sec; △, — — — —, $U = 1$ ft./sec; □, – – – –, $U = 2$ ft./sec; ▽, ———, $U = 3$ ft./sec. $c_0 = 0{\cdot}023$, $c_1 = 0{\cdot}042$, $c_2 = 0{\cdot}034$, $\alpha = \pi$.

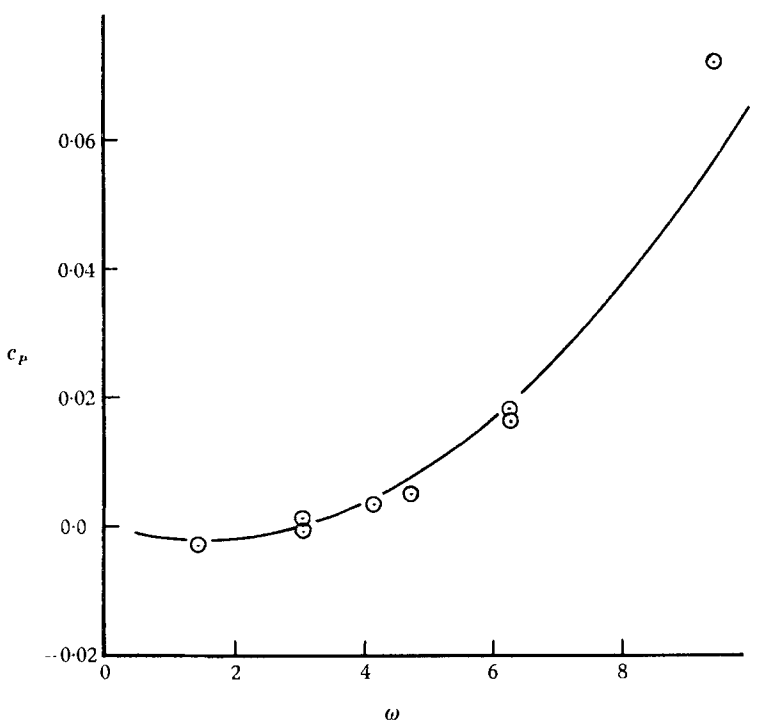

FIGURE 12. Power coefficient versus reduced frequency for quadratic amplitude. $c_0 = 0{\cdot}023$, $c_1 = 0{\cdot}042$, $c_2 = 0{\cdot}034$, $\alpha = \pi$. Theory: Siekmann (1963). Experiment: rubber hydrofoil, ⊙.

(*b*) *Three-dimensional flow*

The cited theoretical investigations were developed for two-dimensional flow. An attempt was made to ensure this in the experiments by placing two vertical walls, one on either side of the foil. However, seven pairs of slots $\frac{1}{2}$ in. wide by 3 in. long were cut in the walls to allow access to the plate by the driver arms.

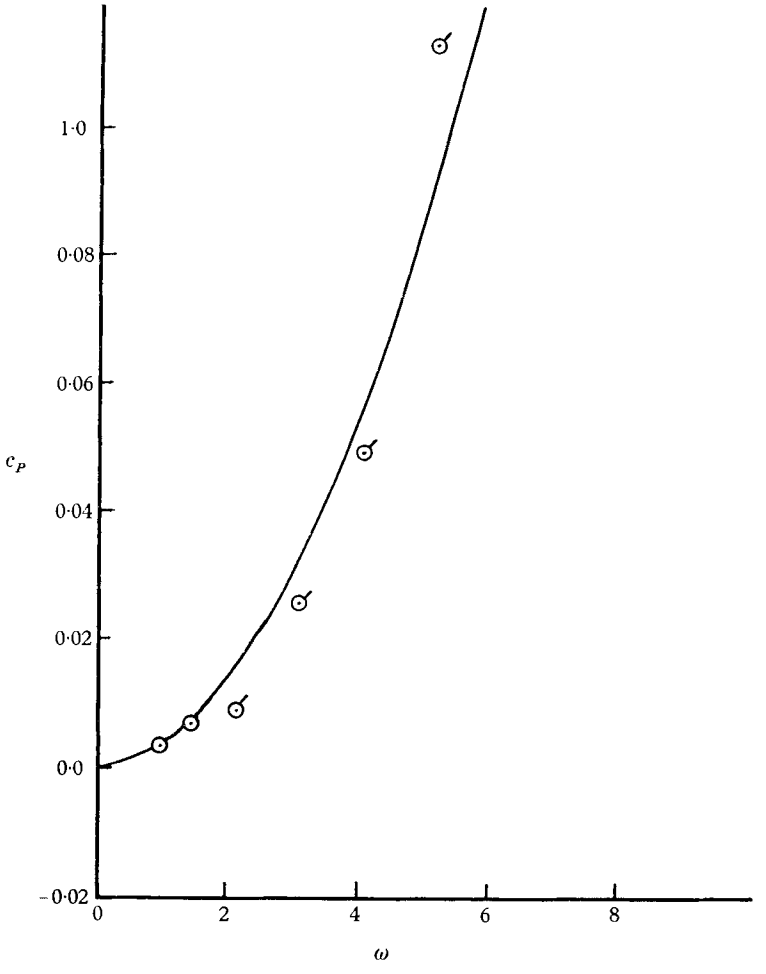

FIGURE 13. Power coefficient versus reduced frequency for constant amplitude. $c_0 = \frac{1}{24}$, $c_1 = 0$, $c_2 = 0$, $\alpha = \pi$. Theory: Siekmann (1963). Experiment: metal hydrofoil, ⊙.

Approximately $3\frac{1}{2}$ in. of the 12 in. chord was open-ended. It is possible that flow would develop around the edge of the foil from the positive to the negative pressure side resulting in a lower experimental thrust reading for a given set of conditions. Increasing the width or aspect ratio of the hydrofoil would decrease the magnitude of this effect.

(*c*) *Extraneous drag*

The strain-gauge records of thrust versus time for no water around the plate, as shown in figures 9*a*, *b*, indicate a large extraneous periodic force (indicated by the dotted line) arising somewhere in the mechanism upon which the thrust output of the plate is imposed (solid line). During the first series of runs it was noted that the driver arms were striking the edge of the slots in the wall and that the drag-link arm occasionally struck against the support structures when the model was being operated with the wavelengths $\lambda = 2$ and 4 ft. These defects were corrected and have no bearing on the strain-gauge records shown. The driver arms were held in place by Teflon buttons on the outside which rubbed against the outside plastic wall. Under static conditions it was noted that the starting force required to slide the hydrofoil in a fore- and aft-direction was less than 0·030 lb. With a small amount of vertical velocity in the driver rods, this dropped to less than 0·010 lb., which is approximately $\frac{1}{20}$ the size of the peak-to-peak forces noted in the no-water condition for the hydrofoil, according to the strain-gauge traces. The magnitude of these forces does not appear to be frequency-dependent, though their period follows that of the basic machine period exactly.

Additional experimental effort would be required to determine the source of this force and to eliminate it from the apparatus. In view of the erratic behaviour of the thrust versus time strain-gauge traces it was decided to include table 1, detailing correlation between the mechanical balance and the strain gauge. The agreement between the mechanical balance and the strain-gauge determination of the time average thrust is good. The mechanical balance was massive, had a resonant frequency of less than 1 c/s, and performed its own integration of the thrust input.

(*d*) *Flow errors*

While the flow meter apparatus could determine the flow velocity at the propeller location to within $\pm 2\,\%$, its readings were open to question. The location selected for the propeller was halfway between the model wall and the tunnel wall and a lifter to the rear of the model. If the tunnel flow rate was 0 or 1 ft./sec and the model was set operating at 6 c/s, a flow was induced by the pumping action of the plate between the two vertical walls of the model, raising the question as to what the correct experimental flow velocity was. Some measurements of the wake velocity aft of the plate were made using the 1 in. diameter propeller meter and found to be equal to the wave velocity of the foil.

Thrust coefficients determined with $U = 2$ ft./sec and $U = 3$ ft./sec agreed well with one another. For $U = 1$ ft./sec it turned out that the experimental data did not agree satisfactorily with the other ones. They usually lay along a line parallel to and displaced in a random manner slightly above or below the $U = 2$ ft./sec and 3 ft./sec data.

(*e*) *Power data*

As noted earlier, the power required to drive the hydrofoil in water for given sets of test conditions was taken as the difference between the power required to drive the entire machine with the hydrofoil in water and the power required to

drive the entire machine with the hydrofoil out of the water. This net power difference was small in comparison with the gross power requirements of the machine. Small variations in the gross requirements of the machine would introduce large errors into the derived power requirements of the hydrofoil.

$c_0 = 0{\cdot}023$, $c_1 = 0{\cdot}042$, $c_2 = 0{\cdot}034$, $\alpha = \pi$

Run	U (ft./sec)	c/s	Thrust (lb.) Mechanical balance	Thrust (lb.) Strain gauge	Torque (ft. lb.)
293	no water	1·0	0·0	0·007	0·926
294	—	1·0	0·0	0·007	0·945
295	—	2·0	0·0	0·000	0·952
296	—	3·0	0·0	0·000	0·957
297	—	4·0	0·0	0·005	0·922
298	—	5·0	0·0	0·000	Osc. no trace
299	—	6·0	0·0	0·000	No trace
301	0	1	0·0	0·011	0·85
302	0	2	0·019	0·0262	0·938
303	0	3	0·036	0·0452	0·966
304	0	4	0·063	0·0592	1·02
305	0	5	0·096	0·092	Osc.
306	0	6	0·136	0·134	1·153
307	1	1	−0·005	+0·00463	0·922
308	1	2	+0·012	0·0194	0·959
309	1	3	+0·024	0·0265	1·058
310	1	4	+0·044	0·049	1·023
311	1	5	+0·071	0·078	Osc.
312	1	6	+0·109	0·118	1·165
315	2	1	−0·038	−0·0285	—
316	2	2	−0·018	−0·016	—
317	2	3	−0·004	−0·005	—
318	2	4	+0·010	+0·013	—
319	2	5	+0·030	+0·030	—
320	2	6	+0·057	+0·056	—
333	3	1	−0·097	0·084	—
334	3	2	−0·070	0·065	—
335	3	3	−0·055	0·056	0·98
336	3	4	−0·037	0·035	1·015
337	3	5	−0·010	0·009	Osc.
338	3	6	+0·012	+0·013	1·105

TABLE 1. Comparison of integrated strain-gauge thrusts versus mechanical balance readings

This problem may be corrected only by increasing the ratio of hydrofoil power to machine power. Since the machine is operating near its minimum power requirements, this leaves increasing power absorbed by the hydrofoil as the only alternative. Increasing the area of the hydrofoil by doubling its width or increasing the flow velocity with reduced frequency to be held constant would accomplish this. The latter series of tests were conducted with a maximum flow velocity of

3 ft./sec. Flow velocities of about 8 ft./sec would impose loads approximately seven times as large on the apparatus as the 3 ft./sec flow; however, it is believed that the machine is capable of withstanding these considerably larger loads when one of the moulded rubber hydrofoils would be employed.

8. Conclusion

On the interval of reduced frequency on either side of $\omega = \pi$ for which experimental conditions fulfilled the basic assumption that the perturbation velocities are small compared with the free-stream velocity, good agreement between theoretical and experimental thrust coefficients was achieved. This was especially true for the cases of constant and quadratic amplitudes. In the case of the linear amplitude, an additional small discrepancy was noticed which could have originated from any one of several sources. Additional testing would be required to isolate its cause.

As the reduced frequency ω becomes larger than 6, the assumption that the flow field can be represented by linearized Euler equations is no longer valid. A solution of the full non-linear equations of motion would be required before further conclusions could be drawn.

The series of tests described in the present paper were intended to determine the suitability of linearized, two-dimensional theories for predicting the thrust and power properties of a travelling wave hydrofoil in two-dimensional flow. In this it has succeeded. The final goal, of course, is to develop a three-dimensional theory which will allow one to predict the thrust produced and power requirements of a three-dimensional body such as that of a fish. An important theoretical contribution concerning the swimming of slender fish is due to Lighthill (1960). Preliminary results of experimental studies of the hydrodynamic aspects of actual fish propulsion were discussed briefly by Waugh, Kelly & Fabula (1961).

REFERENCES

KELLY, H. R. 1961 Fish propulsion hydrodynamics. *Developments in Mechanics*, vol. 1, pp. 442–50. New York: Plenum Press.

LIGHTHILL, M. J. 1960 Note on the swimming of slender fish. *J. Fluid Mech.* **9**, 305–17.

SIEKMANN, J. 1962*a* Theoretical studies of sea animal locomotion, Part 1. *Ingen.-Arch.* **31**, 214–28.

SIEKMANN, J. 1962*b* Untersuchungen über die Bewegung schwimmender Tiere. *VDI-Zeitschrift*, **104**, 433-9.

SIEKMANN, J. 1963 Theoretical studies of sea animal locomotion, Part 2. *Ingen.-Arch.* **32**, 40–50.

SMITH, E. H. & STONE, D. E. 1961 Perfect fluid forces in fish propulsion: the solution of the problem in an elliptic cylinder co-ordinate system. *Proc. Roy. Soc.* A, **261**, 316–28.

WAUGH, J. S., KELLY, H. R. & FABULA, A. G. 1961 Recent Hydrodynamics Research at the Naval Ordnance Test Station, paper presented at the *Fifth Navy Science Symposium*, Naval Academy, Annapolis, Md., 1961.

WU, T. YAO-TSU 1961 Swimming of a waving plate. *J. Fluid Mech.* **10**, 321–44.

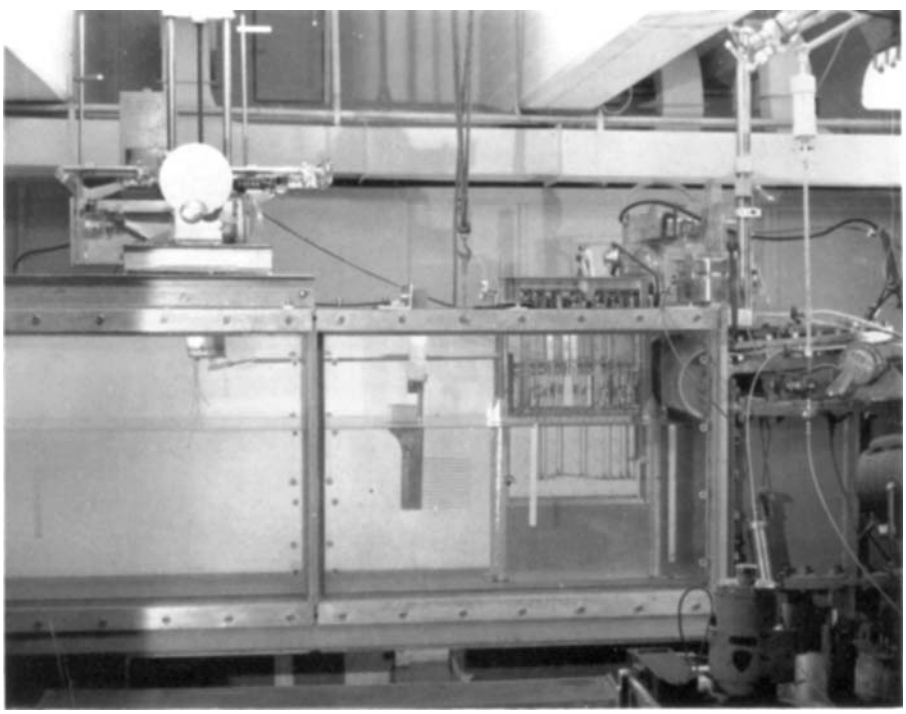

FIGURE 8. Photograph of experimental apparatus (in water tunnel), mechanical balance (upper left) and Pitot rake.